SF2A 2017
C. Reylé, P. Di Matteo, F. Herpin, É. Lagadec, A. Lançon, Z. Meliani, F. Royer (eds)

THE MASS ASSEMBLY HISTORY OF THE MILKY WAY NUCLEAR STAR CLUSTER

A. Mastrobuono-Battisti[1] and A. Tsatsi[1]

Abstract. Nuclear star clusters (NSCs) are dense stellar clusters observed in the center of a large fraction of galaxies, including the Milky Way. Although their evolution is strictly connected to that of their host galaxy, their origin is still unknown. We explore one of the possible formation mechanisms by studying direct N-body simulations of initially randomly distributed globular clusters (GCs) that ispiral to the center of a Milky Way-like nuclear disk. We find that the NSC that forms through this process shows both morphological and kinematical properties that make it comparable with observations of the Milky Way NSC, including significant rotation, a property usually attributed to the infall of gas and following in-situ star formation. We prove that no fine-tuning of the initial orbital distribution of the infalling GCs is necessary to result in a rotating NSC. Therefore, we conclude that the cluster inspiral is a possible mechanism for the formation of the Milky Way NSC and we put constraints on the build up history of the Galactic NSC.

Keywords: Galactic nuclei, Milky Way, nuclear star cluster, formation, kinematics, morphology, globular clusters

1 Introduction

Nuclear star clusters (NSCs) are extremely dense and compact stellar systems, with masses between $\sim 10^6$ $M_\odot$ and 10^7 $M_\odot$, effective radii of a few pc and central luminosities up to $\sim 10^7$ $L_\odot$. They are commonly observed in the nuclei of galaxies along the whole Hubble sequence and they often coexist with a central supermassive black hole (SMBH, see Böker 2010, for an overview). Their properties seem to scale with those of their host galaxies suggesting a close connection between their evolution and the build up of the whole galaxy. However, their formation mechanism is not yet known. Two main hypotheses have been suggested: the in-situ star formation scenario, where gas infalls into the nucleus and forms stars (Schödel et al. 2008) and the inspiral scenario, where massive clusters, like globular clusters (GCs), decay to the galactic center via dynamical friction and merge to form a dense NSC (Tremaine et al. 1975; Capuzzo-Dolcetta 1993). Since both old and young stars are observed in galactic nuclei, these processes are not exclusive and they could work in parallel, contributing to the formation of the NSC. Here and in Tsatsi et al. (2017) we explore and test the merger scenario using detailed N-body simulations of consecutive decays of GCs into a Milky Way (MW) like nuclear disk and compare the results of the simulations to observations, using the MW NSC as a benchmark. In Section 2 we describe our simulations and the method we used for our analysis, in Section 3 we compare our results with observations and we show how kinematic misalignments and substructures could be used to disentangle the different formation mechanisms. In Section 4 we draw our conclusions.

2 Simulations and methods

The N-body simulations used in this study are described in detail in Antonini et al. (2012); Mastrobuono-Battisti et al. (2014) and Tsatsi et al. (2017). In brief, we simulate the formation of a Milky Way-like NSC through the consecutive infall of 12 identical globular clusters (GCs) with a mass of $1.1 \times 10^6 M_\odot$ each, in the inner region of a nuclear disk ($M_{nd} = 10^8 M_\odot$), hosting a central SMBH ($M_\bullet = 4 \times 10^6 M_\odot$)), similar to Sgr A* (Genzel et al. 2010). Each GC is represented by a tidally truncated King (1966) model and is initially moving on a circular orbit with randomly chosen parameters, at a galactocentric distance of 20 pc. The time interval

[1] Max-Planck Instiut für Astronomie, Königstuhl 17, 69117 Heidelberg, Germany

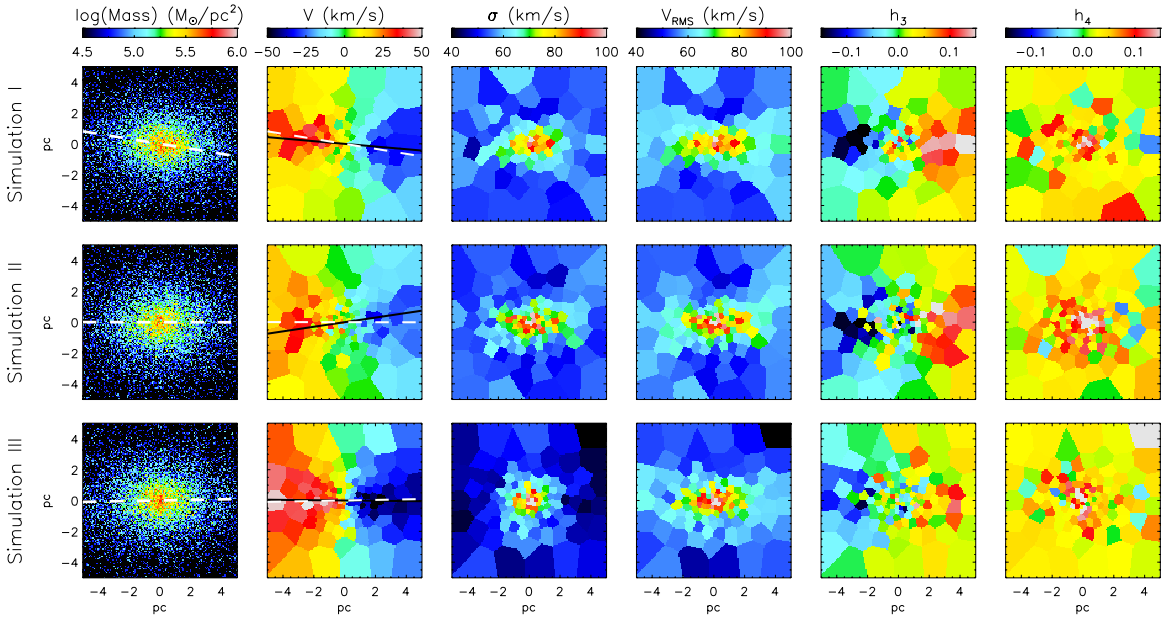

Fig. 1. LOSVD of the simulated NSC. From left to right: Projected stellar mass surface density, line-of-sight velocity v, velocity dispersion σ in km/s, and higher-order moments h_3 and h_4, comparable to the skewness and the kurtosis, respectively. The white dashed line shows the major photometric axis, while the solid black line shows the kinematic major axis of each cluster. From Tsatsi et al. (2017).

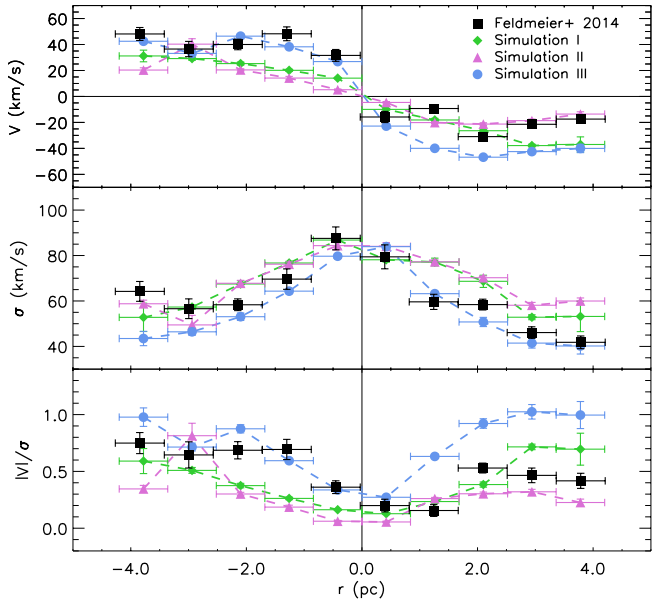

Fig. 2. Kinematic profiles (V, σ and V/σ) for the three simulated clusters (dashed lines) compared to the corresponding profiles of the Milky Way NSC (black squares) by Feldmeier et al. (2014). All profiles are extracted from a slit along the kinematic axis and the asymmetry between left and right side of the MW NSC is caused by dust extinction (Chatzopoulos et al. 2015). From Tsatsi et al. (2017).

is kept constant between each infall (∼0.85 Gyr) and the times are rescaled to the real mass of the particles, as described by Mastrobuono-Battisti & Perets (2013). After the last infall the whole system is evolved in isolation for ∼2.2 Gyr accounting for a total time of ∼12.4 Gyr. The total mass of the resulting NSC is $\sim 1.4 \times 10^7 M_\odot$.

This value is in agreement on the 2-σ level with the mass of the MW NSC ($2.5 \pm 0.6 \times 10^7 M_\odot$), as estimated by Schödel et al. (2014). Here we analyse three realizations of the initial conditions described above, with different random parameters for the initial orbital parameters of the infalling GCs for the orbital parameters used in each simulation. Simulation III differs from Simulations I and II because the inclination of the orbits i is aways $<90°$, so that all the GCs inspiral on prograde orbits. This choice of initial parameters has been made to represent clusters that might have initially formed in the central molecular zone of the MW and thus will share a similar orbital spin. In order to compare the mass and orbital distribution of the simulated NSC with observable properties, we create two-dimensional mock stellar mass and kinematic maps by projecting the stellar particles along a line-of-sight which is perpendicular to the total angular momentum vector of the NSC, meaning that the line-of-sight rotation observed should be maximum. Particles are then binned on a regular grid centerd on the center of mass of the cluster, with a field-of-view (FoV) of 5 pc radius, which is approximately the half-light radius of the MW NSC (Schödel et al. 2014). The half-mass radius of our simulated NSC is approximately 10 pc for all simulation set-ups. We would expect differences between observed half-light and half-mass radius of the MW NSC if the mass-to-light ratio is not constant, as a result of the non-trivial interplay between mass segregation and the presence of young bright stars in the central region (e.g. Paumard et al. 2006). Within 5pc, the simulated NSC matches the observed shape of the surface density distribution of the MW NSC (Antonini et al. 2012). Therefore, we limit our kinematic analysis and comparison to this radial extent. The extracted kinematic maps are spatially binned using the 2D Voronoi binning method (Cappellari & Copin 2003). The mass-weighted line-of-sight velocity distribution (LOSVD) of the cluster is then extracted and fitted with the Gauss-Hermite series (van der Marel & Franx 1993; van de Ven et al. 2006). The mass and stellar LOSVD of the three simulated NSCs are shown in Figure 1.

3 Results and comparison with observations

Using the first and second moments of the intensity distribution of our mock images (see Figure 1), we find the position of the projected major axis and the flattening $q = b/a$ of our simulated NSCs within the adopted FoV of 5 pc radius. The average flattening of the NSC is $q = 0.64$ for Simulation I, and $q = 0.69$ for Simulations II and III. These values are remarkably similar to the observed flattening of the MW NSC, $q_{obs} = 0.71 \pm 0.02$ (Schödel et al. 2014). As seen from Figure 1, the NSC shows a significant amount of rotation, of an amplitude of ~ 40 km/s within 5 pc for Simulation I and II. The velocity is higher (~ 50 km/s) for Simulation III, where the infalling GCs have a similar initial orbital direction. In order to compare our results with the observed kinematic profiles of the MW NSC, we estimate the kinematic major axis of the NSC within the adopted FoV using the kinemetry method, as developed by Krajnović et al. (2006). The kinematic axis for each simulated NSC is shown in Figure 1 (solid black lines). We then place a mock slit along the kinematic axis, of width of 0.84 pc and extract the LOSVD of the simulated clusters in equal-size bins of 0.84 pc size, which corresponds to a binning similar to the one used by Feldmeier et al. (2014) to the MW NSC. The corresponding errors are calculated by Monte Carlo simulations of the extracted LOSVD (see van de Ven et al. 2006). The profiles of V, σ and V/σ for the three simulations are shown in Figure 2. The kinematic profiles show a very good agreement with the kinematic profiles observed in the MW NSC (Feldmeier et al. 2014).

3.1 Kinematic misalignments and substructures

Figure 1 shows the measured kinematic and the photometric major axes of all simulated NSCs within the adopted FoV. We find that the offset between these two axes within 5 pc is $\Delta\theta \sim 4.2°$, $8.6°$ and $0.5°$ for Simulations I, II, and III, respectively. Simulation I also shows a misalignment of about $9.2°$ between the photometric major axis within 5 pc and the projected plane, which is perpendicular to the total angular momentum vector of the NSC (the x axis of Figure 1). Simulation III, however, characterised by inspiralling GCs with similar orbital directions, shows no significant offset between the kinematic and the photometric axis of the resulting NSC. A misalignment of $\sim \Delta\theta \sim 9° \pm 3°$ between kinematics and morphology has also been recently observed in the MW center suggesting this as an evidence that cluster-inspirals may have played a role in the formation of the MW NSC (Feldmeier et al. 2014). Here we confirm that this scenario is able to produce observable misalignments between the photometry and kinematics of the resulting NSCs, which are stronger in the case where the infalling GCs have initially random orbital spin orientation (Simulations I and II), however not in the case where the GCs infall with a similar orbital direction (Simulation III). Moreover, the detailed study of the internal kinematics can provide an important tool to disentangle the possible formation mechanisms. Indeed, recent findings by Feldmeier et al. (2014) provide strong evidence for a kinematic substructure in the MW NSC,

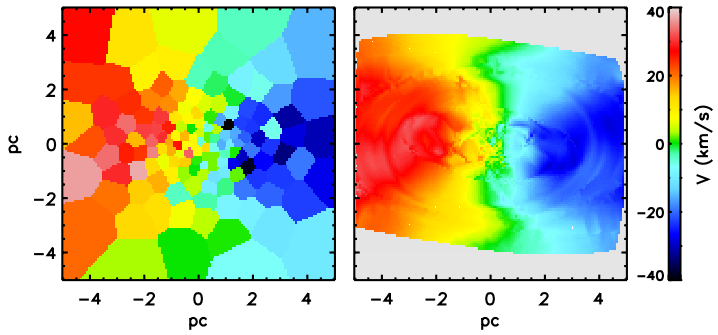

Fig. 3. Left: Mock line-of-sight velocity map of the NSC of Simulation II, after the infall of the 12th GC. Right: the corresponding kinemetric model, showing a weak polar twist at ∼3 pc. From Tsatsi et al. (2017).

rotating perpendicularly to its main body, which can be interpreted as a fossil record of a past merger event. In order to study the role of mergers in creating such kinematic substructures, we use the apply the kinemetry method to our simulated kinematic maps. In this way, we find a substructure (see Figure 3) created by a past polar merger event of a globular cluster. This is a merger signature that can be observable and long-lasting (for 3 Gyr) in the kinematics of the NSC.

4 Conclusions

We explored the possibility of a merger origin of NSCs, using N-body simulations of the consecutive inspiral of GCs in the center of a MW-like nucleus. We find that even if the GCs are initially randomly distributed around the center, the resulting NSC shows a significant amount of rotation, and that both its morphological and kinematic properties are comparable to the MW NSC. Moreover, our adopted model can account for observable kinematic misalignments and substructures in the final NSC, that can serve as long-lasting fossil records of past merger events. This is in line with recent observations of a similar substructure in the MW NSC (Feldmeier et al. 2014). According to our results, the cluster infall scenario is a viable hypothesis for NSC formation. However, the search for the dominant formation mechanism of NSCs is still ongoing, and clarifying the nature of the Milky Way and extragalactic NSCs formation requires a more detailed study of their dynamics, their stellar populations and star formation history, combined with more realistic simulations of their formation.

References

Antonini, F., Capuzzo-Dolcetta, R., Mastrobuono-Battisti, A., & Merritt, D. 2012, ApJ, 750, 111
Böker, T. 2010, in IAUS, Vol. 266, IAUS, ed. R. de Grijs & J. R. D. Lépine, 58–63
Cappellari, M. & Copin, Y. 2003, MNRAS, 342, 345
Capuzzo-Dolcetta, R. 1993, ApJ, 415, 616
Chatzopoulos, S., Gerhard, O., Fritz, T. K., et al. 2015, MNRAS, 453, 939
Feldmeier, A., Neumayer, N., Seth, A., et al. 2014, A&A, 570, A2
Genzel, R., Eisenhauer, F., & Gillessen, S. 2010, Reviews of Modern Physics, 82, 3121
King, I. R. 1966, AJ, 71, 64
Krajnović, D., Cappellari, M., de Zeeuw, P. T., & Copin, Y. 2006, MNRAS, 366, 787
Mastrobuono-Battisti, A. & Perets, H. B. 2013, ApJ, 779, 85
Mastrobuono-Battisti, A., Perets, H. B., & Loeb, A. 2014, ApJ, 796, 40
Paumard, T., Genzel, R., Martins, F., et al. 2006, ApJ, 643, 1011
Schödel, R., Merritt, D., & Eckart, A. 2008, Journal of Physics Conference Series, 131, 012044
Schödel, R. et al. 2014, A&A, 566, A47
Tremaine, S. D., Ostriker, J. P., & Spitzer, Jr., L. 1975, ApJ, 196, 407
Tsatsi, A., Mastrobuono-Battisti, A., van de Ven, G., et al. 2017, MNRAS, 464, 3720
van de Ven, G., van den Bosch, R. C. E., Verolme, E. K., & de Zeeuw, P. T. 2006, A&A, 445, 513
van der Marel, R. P. & Franx, M. 1993, ApJ, 407, 525